Applied Clay Science 104 (2015) 196–204

Contents lists available at ScienceDirect

Applied Clay Science

journal homepage: www.elsevier.com/locate/clay

Research paper

Occurrence of iron and aluminum sesquioxides and their implications for the P sorption in subtropical soils

Edson C. Bortoluzzi [a,*], Carlos A.S. Pérez [a], José D. Ardisson [b], Tales Tiecher [c], Laurent Caner [d]

[a] Laboratory of Land Use and Natural Resources, University of Passo Fundo, 99001-970 Passo Fundo, Rio Grande do Sul (RS), Brazil
[b] Laboratory of Applied Physics, Center of Development and Nuclear Technology — CDTN, Belo Horizonte, 31270-901 Minas Gerais, Brazil
[c] Department of Soil Science, Universidade Federal de Santa Maria — UFSM, 97105-900 Santa Maria, Rio Grande do Sul, Brazil
[d] Université de Poitiers, IC2MP-HydrASA UMR 7285, TSA 51106, 86073 Poitiers, France

ARTICLE INFO

Article history:
Received 9 June 2014
Received in revised form 7 November 2014
Accepted 22 November 2014

Keywords:
Anion exchange resins
Ferrihydrite
Phosphorus desorption
Soil oxides
X ray diffraction

ABSTRACT

The effect of the pedo-climatic variation in qualitative and quantitative soil sesquioxide contents and soil phosphorus (P) sorption capacities has been studied. In four soils (samples from A horizons) located along a southern Brazilian environmental gradient (EG) shown a decrease in crystallized iron oxides with the increase of altitude. Hematite and goethite were found at low EG altitudes in association with low soil organic carbon content, and goethite–ferrihydrite and gibbsite were found at high altitudes in association with high organic carbon content. The adsorbed soil P (measured by the remaining P) was predicted by the goethite content, and the desorbed P (measured by successive P extractions using anion exchange resin membranes) was predicted mainly by the goethite and clay content. In subtropical soils, even a smooth environmental gradient could determine the qualitative and quantitative iron and aluminum sesquioxide distributions that control soil P sorption capacities.

1. Introduction

Environmental gradient studies can provide very powerful tools for understanding soil weathering and properties primarily when they occur over a similar parent material (Lair et al., 2009; Rasmussen et al., 2010). According to the soil position on the landscape (i.e., the altitude, topography, and parent material) and soil weathering, several mineral species can coexist in different proportions to provide specific soil properties. Besides, the organic matter is also very sensitive to these factors. One of the most important soil properties affected by the mineral composition and organic matter content is the phosphate (P) adsorption and desorption capacities, which play an important role in both agronomic and environmental aspects (Bortoluzzi et al., 2013). Thermodynamically, all P adsorbed into the soil can be desorbed (Barrow, 1983); however, the kinetics of desorption ability depends largely on the soil mineralogy, particularly the Fe and Al oxides, clay and carbonates (Chintala et al., 2014).

Goethite, hematite, lepidocrocite, and ferrihydrite are the most common species in soils (Dixon and Weed, 1989), and their presence is in accordance to the soil evolution conditions (Schwertmann and Kämpf, 1983; Kämpf et al., 2009). Ferrasols located near the Equator primarily contain gibbsite, and tropical and subtropical Ferralsols primarily exhibit hematite, goethite, maghemite, and magnetite (Ferreira et al., 2003). Ferrihydrite and lepidocrocite are found in poorly drained soils (Schwertmann and Kämpf, 1983), exhibiting higher P adsorption and a faster adsorption rate (Wang et al., 2013). Goethite occurrence is favored by high soil organic carbon content and low pH (Kämpf et al., 2009), and usually has a higher relative affinity for P than hematite (Guzman et al., 1994). Compared to kaolinite, goethite has a much higher P adsorption capacity, because the ≡Fe – OH groups are spread over the entire surface of goethite while ≡Al – OH groups on the surface of kaolinite are located exclusively at the edges of the crystal structure (Wei et al., 2014). Even though, recent works show an unexpected high contribution of clay minerals in P adsorption, especially in the less acidic conditions (Devau et al., 2009).

In Southern Brazil, the main soils are primarily Ferralsol types, and their mineralogy is dominated by large amounts of Fe and Al sesquioxides, kaolinite-group clay minerals (Paduani et al., 2009), and 2:1 clay type with hydroxy-Al interlayers (Bortoluzzi et al., 2008; Caner et al., 2014). These soils are acidic under natural conditions, facilitating specific P sorption, forming preferentially bidentate binding with both iron (Kim et al., 2011) and aluminum oxides (Li et al., 2013). In a numerical modeling study, Devau et al. (2009) showed that the concentration of P adsorbed onto Al- and Fe-oxides increased in the acidic domains, where these minerals contributed to as much as 50% of the total adsorbed. Indeed, the P retention in tropical and subtropical soils by Fe and Al oxides is one of the most limiting factors for crop production (Igwe et al., 2010). De Mesquita Filho and Torrent (1993) showed that in high weathered Ferralsols the P sorption is related most to the

* Corresponding author. Tel.: +55 54 33 16 81 51.
E-mail address: edson.bortoluzzi@pq.cnpq.br (E.C. Bortoluzzi).

http://dx.doi.org/10.1016/j.clay.2014.11.032
0169-1317/

organic content that based upon mineralogy composition. However, in extensive areas of the Paraná basin (Southern Brazil) under subtropical condition, less weathered soils are found and their mineralogy is diversified. Marked differences in soil sesquioxide mineral compositions can occur in response to the environmental gradient in which the soil phosphorus sorption phenomena should be studied. It is particularly interesting because, regardless of the soil mineralogy, the phosphate fertilization recommendation is based on the soil clay content alone (Comissão de Química e Fertilidade do Solo — CQFS-RS/SC, 2004) and the mineralogical approach makes up an excellent way in soil studies under agronomic and environmental aspects (Bortoluzzi et al., 2013).

In this sense, the objectives of this work were to estimate how the environmental gradient in the basaltic plateau of the Rio Grande do Sul State of southern Brazil controls iron and aluminum sesquioxide and clay mineral distribution in the soils, and the subsequent impact of these quantities on soil phosphate adsorption and desorption capacities. This approach may further elucidate the impact of soil mineralogy on soil P sorption, which has both agricultural and environmental importance.

2. Material and methods

2.1. Site descriptions and soil sampling

This study was conducted in the southern Paraná Basin, Rio Grande do Sul State, Southern Brazil (Fig. 1). The geological formation is from the Mesozoic era (volcanism). Basaltic flow thicknesses ranging from 20 to 1200 m occur at the bottom of the pile (western region) above sedimentary rocks (sandstone), and alkaline basaltic lava flows are observed at the middle position; basaltic-andesite, rhyolite and rhyodacite are on the top of the formation (eastern region).

The region experiences a subtropical humid climate and a wavy relief covered with natural pastures in the upper portion of the landscape with natural forest in the lower portion of the landscape. Table 1 shows the main characteristics of the soil sampling sites, including geographic location, soil/land use, profile attributes and, few soil attributes. The soils are predominately developed on basaltic rock and they are classified as Latossolos and Cambissolos by the Brazilian System of Soil Classification or Ferralsol/Cambisol in the World Reference Base for Soil Resources (IUSS Working Group, 2007). The soils are used as intensive agriculture, but remains little areas with the natural vegetation or with low anthropogenic pressure. The soils are highly weathered and show deep profiles (1–4 m). They are well drained, with a horizon sequence that comprises A-Bw/Bi-C-R horizons or layers. The Bw horizon is found in the Ferralsol and the Bi horizon is in the less developed Cambisol. Regosols (A horizon upper R) are only found in the steep slopes.

Four sites under natural vegetation were chosen along the environmental gradient from west to east in Rio Grande do Sul State (Fig. 1). There are large variations in the environmental conditions (altitude, mean annual temperature, and precipitation) across the gradient. The altitude ranges from 220 to 1,080 m above sea level, the maximum air temperature vary from 21 to 25.9 °C, and the total annual precipitation ranges from 1 688 to 1 792 mm (Table 1).

In each site on the same soil type, three subsamples (approximately 5 kg of soil each) were collected with both preserved and non-preserved structures. For each subsamples with non-preserved structure, 10 subsamples around a central point were collected at 0–20 cm depth. The non-preserved structure samples were air-dried, and an aliquot was sieved at 2 mm to obtain air-dried fine earth (ADFE).

2.2. Soil characterization

The soil color was estimated using a Munsell soil color chart. Total organic carbon (TOC) content was determined by wet oxidation with $K_2Cr_2O_7$ and H_2SO_4 (Walkley and Black, 1934), with modifications proposed by Tedesco et al. (1995). Briefly, 0.25 g of soil was weighted in glass tubes (25.0 cm length × 2.5 cm diameter) with 10 mL 0.067 mol L^{-1} $K_2Cr_2O_7$ and 15 mL H_2SO_4 concentrate. The tubes were placed in a digestion block at 150 °C for 30 min. After, the content in the tubes was transferred to erlenmeyers where it was added 80 mL distilled water. Then, the amount of $Cr_2O_7^{2-}$ not reduced was obtained by titration with Fe^{2+} [0.2 mol L^{-1} $Fe(NH_4)_2(SO_4)_2.6H_2O$] in the presence of ferroin indicator. Finally, the content of carbon obtained was corrected to the content of carbon obtained by dry combustion (elementary analyzer) using the correction factor of 1.14, as proposed by Rheinheimer et al. (2008). pH measurements were performed in a 1:1 soil:water ratio. Exchangeable $H^+ + Al^{3+}$ were estimated by solving with the following equation: $H + Al = e^{10.665 - 1.1483SMP}/10$ (Kaminski et al., 2001), where SMP is the pH measurement in aqueous suspension using SMP buffered solution at pH 7.5 (triethanolamine, paranitrophenol, K_2CrO_4, $Ca(CH_3COO)_2$ and $CaCl_2.2H_2O$) (Shoemaker et al., 1961).

The particle size distribution was determined after chemical dispersion using NaOH solution (6% *w*/*w*) and mechanical shaking. The sand fractions were separated by sieving and then weighed, and the silt and clay fractions were separated by sedimentation, with clay content quantification by the pipette method. The soil bulk density was determined soil with preserved structure, using volumetric rings (5 cm × 5 cm). The total specific surface area (SA) was gravimetrically estimated using ethylene glycol monoethyl ether (EGME) adsorption on the soil

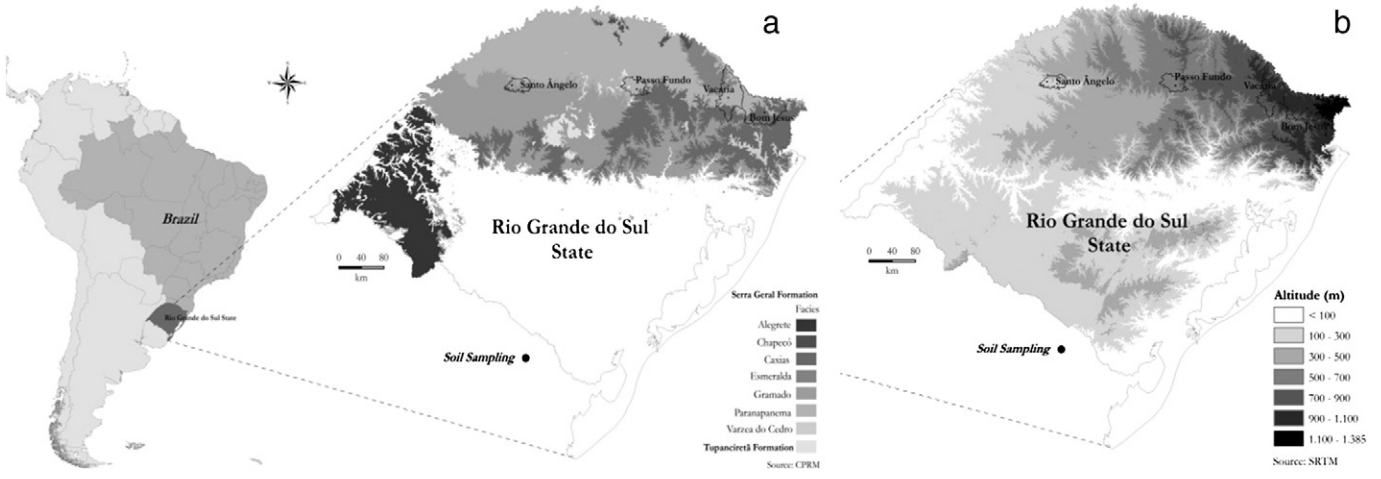

Fig. 1. Map showing the collection sites in the context of the: a) geological formation, b) altitude.

Table 1
Site locations, environmental characteristics and soil chemical and physical properties.

Explanatory variables	Sites			
	Bom Jesus	Vacaria	Passo Fundo	Santo Ângelo
	SBJ	SV	SPF	SSA
Climatic and topographic attributes				
Geographic direction	East			West
Geographic coordinates	50° 26′ W	51° 01′ W	52° 28′ W	54° 25′ W
	28° 39′ S	28° 25′ S	28° 19′ S	28° 15′ S
Altitude a.s.l., m	1080	900	590	220
Average max temperature, °C	21.0	21.6	24.4	25.9
Annual rainfall, mm	1792	1700	1661	1688
Soil characterization [a]				
Soil types	Cambisol	Ferralsol	Ferralsol	Ferralsol
	Alumic	Alumic, ferric	Dystric, humic	Dystric, ferric
Horizon sequence	A-Bi-R	A-Bw-C	A-Bw-C	A-Bw-C
Lithology	Rhyolite–basalt	Basalt	Basalt–sandstone	Basalt
Profile positions	Hilltop	Hilltop	Hilltop	Hilltop
Predominant declivity, %	5–15	5–10	5–8	8–10
Soil use/vegetation	Grassland/perennial crops	Grassland Annual crops	Annual crops	Annual crops
General soil attributes				
Soil sample colors[b]	10YR 3/1	7.5YR 5/2	5YR 4/3	2.5YR 4/8
TOC, mg kg^{-1}	42.7 ± 6.2	41.5 ± 3.8	30.6 ± 7.6	24.4 ± 7.6
Soil bulk density, Mg m^{-3}	1.16 ± 0.15	1.66 ± 0.25	1.20 ± 0.17	1.54 ± 0.17
Specific surface area, m^2 g^{-1}	92.3	106.7	87.7	68.5
Particle size distribution				
Sand, g kg^{-1}	138	203	569	221
Silt, g kg^{-1}	256	234	149	151
Clay, g kg^{-1}	606	563	282	628
Chemical attributes				
pH water, 1:1 *v/v*	4.5	5.2	4.8	5.6
$H^+ + Al^{3+}$, $cmol_c$ kg^{-1}	10.4	2.9	3.1	2.0

[a] Soil profile characterization.
[b] Soil colors were estimated using the Munsell color chart; a.s.l. means above sea level; and TOC is the total organic carbon content. Specific surface area measured by EGME (Carter et al., 1965).

particles (Carter et al., 1965). The soil characterization is summarized in Table 1.

2.3. Mineralogical analysis

The chemical elemental composition was determined by Energy Dispersive X-ray Fluorescence Spectroscopy (EDXRF) on a Shimadzu Ray EDX-720 device. The samples were dried at 60 °C, milled in a mortar and placed in containers with filters (3518 Mylar 0.25-mil, 6 μm). Chemical elements are expressed in oxide mass percentages; those with a relative contribution below 0.1% were not considered. In addition, the $R^{3+}/R^{3+}+R^{2+}+M^{+}$ (weathering index) was calculated according to Meunier et al. (2013). For this purpose, M^{+} was calculated by adding the Na^{+}, K^{+}, and $2Ca^{2+}$; R^{2+} was calculated by taking the sum of Mn^{2+}, Mg^{2+}, and Fe(II), and R^{3+} was calculated by adding up the Fe(III) and Al^{3+} (expressed in molar proportions).

Crystalline forms of Fe oxyhydroxides (Fe_d) were estimated by extraction with dithionite–citrate–bicarbonate (DCB) (Mehra and Jackson, 1960); amorphous and/or poorly crystallized forms of Fe (Fe_o) were estimated by extraction with 0.2 mol L^{-1} ammonium oxalate at pH 3 (Blakemore et al., 1987). Extracted elements were determined by ICP OES. The results are presented as Fe_d/Fe_o ratios and Fe_d–Fe_o values to estimate well-crystallized Fe-oxides. Fractions lower than 50 μm were also submitted for DCB treatment and named $Al_{d<50}$, $Fe_{d<50}$, and $Si_{d<50}$.

The soil clay fractions were analyzed by X-ray diffraction (XRD) using a Philips diffractometer model PW1830/25 with CuKα radiation (λ = 0.154 nm). The XRD patterns were performed on non-oriented powder samples and recorded between 2 and 80°2θ.

Mössbauer measurements were performed on the clay fractions at room temperature (RT) and at 20 K with a ^{57}Co/Rh source on a conventional Mössbauer spectrometer operating in constant acceleration mode. A velocity calibration was performed at RT with a α-Fe absorber; all isomer shifts (IS) are referred to this standard. The Mössbauer spectra consist of a paramagnetic component (doublet) mingled with a magnetic phase, and they are represented by a subspectrum of six lines (sextet). The corresponding hyperfine parameters were obtained from the following fitting procedure: hyperfine magnetic field (B_{hf}), quadrupole splitting (EQ), and quadrupole doublet line width (Lorentzian linewidth, Γ). The doublet may be associated with the presence of Fe in silicates (substituting Al with Fe in tetrahedral sites) and/or the presence of iron oxides in a superparamagnetic state.

The magnetic fraction can be attributed to iron oxides present in the samples. The relative contribution of the magnetic sub-spectrum (relative surface area) varies from one sample to another. In natural environments, iron oxides often display a broad particle size distribution at the nanometer scale that induces a phenomenon called superparamagnetism. This phenomenon is characterized by the spontaneous reversal of the magnetization direction of the particles, and it is directly associated with their size. For example, superparamagnetism occurs at RT for hematite particles smaller than 8 nm and for goethite particle smaller than 20 nm (Murad, 2013).

2.4. P sorption phenomena: adsorption and desorption

The soil P maximum sorption capacity was performed by adding 5 ml of a solution containing 0.01 mol $CaCl_2$ L^{-1} and 60 mg of P L^{-1} at pH 5.5 (using K_2HPO_4 as the P source) into a centrifuge tube containing 0.5 g of soil. The samples, in triplicate, remained under continuous shaking at 33 rpm with an end-over-end agitator for 3 days at 20 °C (±2 °C), in an adaptation from Alvarez et al. (2000). After P saturation, the samples were centrifuged at 5000 rpm for 15 min to sediment the particles,

and the supernatant was then filtered at 0.22 μm to eliminate dispersed fine particles. In the supernatant, the remaining P (Prem) was determined by spectrophotometry according to the method proposed by Murphy and Riley (1962).

The P soil desorption capacity was subsequently estimated by successive extractions with anion exchange resin (AER) membrane. All tubes contained 0.5 g of soil and 15 mL of osmosed water (MilliQ® quality, at pH 9.0) received one AER membrane previously saturated with $NaHCO_3$ 0.5 mol L^{-1}. The suspensions were stirred for 18 h at 33 rpm in an end-over-end stirrer at 20 °C (± 3 °C). The AER membranes were then removed and washed with osmosed water flush and then eluted at 10 ml HCl 0.5 mol L^{-1} for 30 min under agitation. Then, the P concentrations in the acid extract were also determined as mentioned early (Murphy and Riley, 1962). The AER, after P extraction, were regenerated by three successive washings with HCl 0.5 mol L^{-1} and saturated with with $NaHCO_3$ 0.5 mol L^{-1} for a new use. A total of seven P extractions were performed and a curve obtained with the cumulative values of desorbed P (mg P kg^{-1} of soil) was fitted using the software SAS (1992) with the following first-order kinetic equation as proposed by McKean and Warren (1996):

$$P_{desorbed} = \beta - (\beta - a)e^{-ht} \quad (1)$$

where β is the maximum amount desorbed or potentially available P, α is the amount of P desorbed in the first extraction, λ is the desorption rate constant, and t is the extraction time. The α and β parameters were adjusted to the clay content (mg P kg^{-1} of clay). The easily desorbable P was estimated as the ratio of α^*100/β.

2.5. Statistical analysis

Pearson correlation coefficients (r) were performed among environmental and soil attributes. The number of soils ($n = 4$) and repetitions ($n = 3$) was low. Even though, we performed correlation analysis as an exploratory analysis to evaluate some trends that were discussed in the manuscript. The data will be presented and discussed in consideration of the soil attributes to highlight the environmental gradient conditions and the iron sesquioxide contents.

3. Results

3.1. Soil chemical attributes along the environmental gradient in southern Brazil

The environmental gradient induced substantial variations in soil attributes, such as the specific surface area (68.5 to 106.7 $m^2\ g^{-1}$), the pH in water (from 4.2 to 5.6), the potential acidity expressed by the exchangeable $H^+ + Al^{3+}$ (2.0 to 10.4 $cmol_c\ kg^{-1}$), soil bulk density (1.16 to 1.66 Mg m^{-3}), and soil organic carbon (24.4 to 42.7 mg kg^{-1}) (Table 1). In general, the soil altitude across the environmental gradient seems to be the main factor controlling the soil physical and chemical attributes. The clay fraction dominated the particle size distribution from soils, ranging from 282 to 628 g kg^{-1}, except for the SPF site in which the sand fraction is higher (569 g kg^{-1}) because of the presence of basalt and sandstone as parent material (Table 1). The soils located at low altitudes (i.e., SPF and SSA sites) are predominantly red (Hue <5YR), indicating the hematite presence, and the value/chroma values observed were high (4/8) indicating the low OC content. At the highest altitude (SBJ site), the yellow color (Hue 10YR) was predominant, indicating goethite presence, and the soils exhibited low value/chroma values (3/1) because of their high OC content. The main total chemical elements, in decreasing order, were SiO_2, Al_2O_3, and Fe_2O_3, with averages of 58.2%, 23.2%, and 13.3%, respectively. The concentrations of CaO, K_2O, and MnO were lower than 1%. Across the environmental gradient, the values for SiO_2 varied from 42.1% to 70.7%; for Al_2O_3 they varied from 19.3% to 26.5%, and in Fe_2O_3, they varied from 5.7% to 24.0%. The other chemical element concentrations were all lower than 5% (Table 2).

The soils from the SBJ and SV sites located at a high elevation exhibited a Fe_2O_3 content of 8.7 and 14.7%, respectively, and the SSA site located at the lowest altitude had a Fe_2O_3 content of 24.0%. The low Fe_o/Fe_d ratios and high Fe_d–Fe_o values at the low altitude (i.e. SSA) indicate the presence of well-crystallized mineral such as hematite and goethite. By contrast, high Fe_o/Fe_d ratios and low Fe_d–Fe_o values were noted at the SBJ and SV sites, indicating the presence of poorly crystallized forms of Fe sesquioxides. The Fe_o/Fe_d ratio tends increase with the increase of altitude and rainfall regime ($r = 0.91$, $P = 0.09$ and $r = 0.92$, $P < 0.08$). All samples exhibited low $Si_{d<50}$ and $Al_{d<50}$ values in the <50 μm fraction. The $Fe_{d<50}$ content in the <50 μm fraction was lower than that of the air-dried fine-earth fraction (ADFE). A major portion of the Fe form is represented by the very well-crystallized form (Fe_d/Fe_o ratio and Fe_d-Fe_o; Table 2).

In Table 2, the $R^{3+}/R^{3+}+R^{2+}+M^+$ weathering index was always higher than 0.9, demonstrating a high degree of soil weathering (Meunier et al., 2013). In addition, this weathering index was affected by the air temperature ($r = -0.91$; $P = 0.09$), rainfall regime ($r = 0.94$; $P < 0.06$), and Fe_o/Fe_d ratio ($r = 0.97$; $P < 0.05$). These findings demonstrate that even under intense weathering conditions, there was great variation in terms of soil chemical composition across the environmental gradient, and they consequently may have different iron mineral species.

3.2. Iron–aluminum sesquioxides in soils along the environmental gradient

The minerals present in the soil samples were characterized by an X-ray diffraction analysis of randomly oriented powders from clay fractions (Fig. 2). All the XRD patterns showed intense peaks at 0.334, 0.424, and 0.182 nm, corresponding to quartz (Qz). Kaolinite (K) was identified by peaks at 0.722, 0.362, and 0.149 nm. The broad

Table 2
Total chemical elements determined by X-ray fluorescence, and weathering indicators of the soil types across an environmental gradient in southern Brazil.

Variable	Site collection			
	Bom Jesus SBJ	Vacaria SV	Passo Fundo SPF	Santo Ângelo SSA
Total elements, %				
SiO_2	62.96	57.11	70.74	42.13
Al_2O_3	24.12	22.78	19.31	26.48
Fe_2O_3	8.71	14.66	5.67	24.02
TiO_2	1.91	2.88	1.59	4.35
SO_3	1.47	1.61	1.71	1.78
CaO	0.31	0.36	0.35	0.34
K_2O	0.22	0.23	0.34	0.20
MnO	0.16	0.15	0.10	0.32
P_2O_5	0.14	0.22	0.18	0.37
Weathering indicators[a]				
Fe_d, g kg^{-1}	22.5	48.0	24.9	59.1
Fe_o, g kg^{-1}	5.3	6.4	2.4	3.6
Fe_d–Fe_o, g kg^{-1}	17.2	41.6	22.5	55.5
Fe_o/Fe_d ratio	0.24	0.13	0.10	0.06
$Fe_{d<50}$, g kg^{-1}[b]	16.1	19.7	2.7	37.3
$Al_{d<50}$, g kg^{-1}	4.4	4.0	1.8	2.3
$Si_{d<50}$, g kg^{-1}	0.33	0.20	0.25	0.38
M^+, %	8.6	9.0	8.0	10.9
R^+, %	2.5	1.3	0.8	3.7
$R^{3+}/R^{3+}+R^{2+}+M^{+c}$	0.96	0.93	0.90	0.95

[a] Each value represents the mean of three replicates. Fe_d and Fe_o were extracted by DCB and oxalate, respectively.
[b] $Fe_{d<50}$, $Al_{d<50}$ and $Si_{d<50}$ are ion extracted in < 50 μm fraction.
[c] $R^{3+}/R^{3+}+R^{2+}+M^+$: weathering index, calculated following Meunier et al. (2013); M^+ is the sum of Na^+, K^+, 2Ca, expressed as a percentage of the concentration (mmol) in relation to the total chemical elements; R^{2+} is the sum of the Mn^{2+}, Mg^{2+}; and Fe(II) and R^{3+} is the sum of Fe(III) and Al^{3+}, both expressed in a percentage of concentration (mmol) in relation to the total chemical elements.

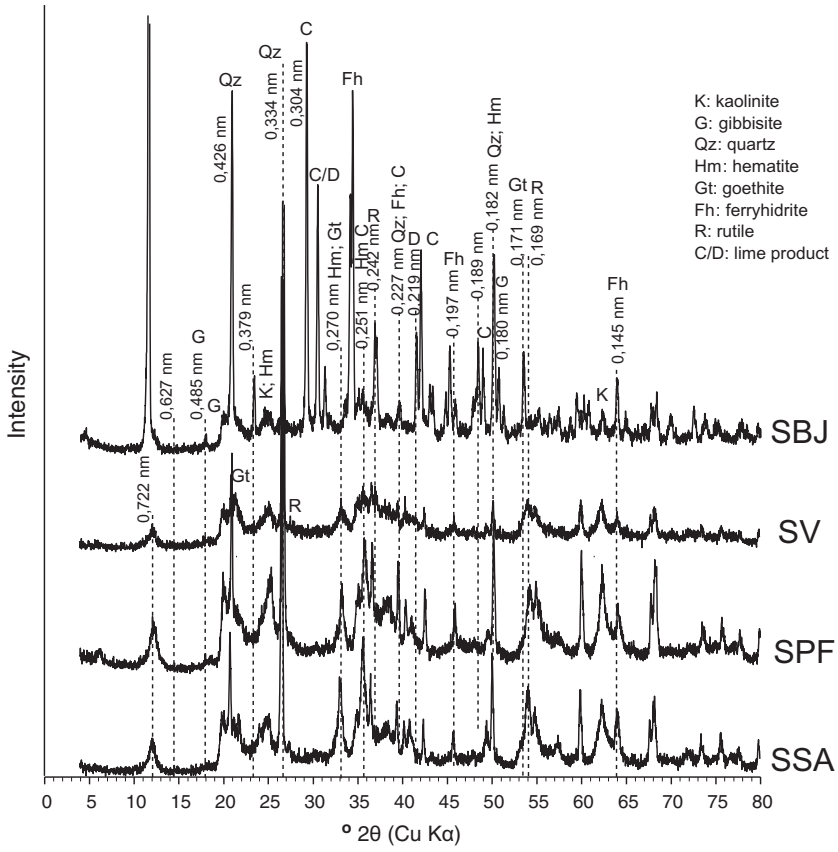

Fig. 2. X-ray diffraction patterns from the clay fraction of the soil types across an environmental gradient in southern Brazil. SBJ is the Bom Jesus site, SV is the Vacaria site, SPF is the Passo Fundo site, and SSA is the Santo Ângelo site.

peaks of kaolinite are indicative of the poorly ordered kaolinite that is a common feature of clay minerals in tropical soils. Gibbsite (G) (0.485, 0.437, and 0.432 nm) was only found in the SBJ and SV samples. Rutile (R) was found in the SSA and SV sites as indicated by the weak peaks at 0.325, 0.248, and 0.168 nm. All soil samples exhibited hematite (Hm) and goethite (Gt), as identified by peak series at 0.368, 0.252, and 0.184 nm and 0.420, 0.245, and 0.170 nm, respectively. The intensity of the peak at 0.269 nm gradually decreased from the SSA sample to the SBJ sample (Fig. 2), which could be attributed to the superimposition of the [104] peak of hematite and the [130] peak of goethite. Ferrihydrite (Fh), a poorly ordered iron hydroxide, is identified by peaks at 0.255, 0.224, 0.198, 0.171, and 0.147 nm, with peak widths and intensities depending on the degree of crystallinity (Schwertmann et al., 1982). SBJ present peaks corresponding to calcite (C) and dolomite (D) due to lime product application.

The identification and quantification of iron oxides by XRD analysis are not easy, especially when they are present in mixtures with other minerals such as quartz (Schwertmann et al., 1982). Mössbauer spectroscopy at room temperature (RT) and at 20 K was used to identify the different forms of Fe hydroxides. The spectra were fitted using one doublet and one sextet (Figs. 3 and 4). The hyperfine parameters obtained from the fitting procedure (Table 3) indicate a quadrupole splitting (EQ) associated with doublets ranging from 0.57 to 0.61 mm s^{-1}, and isomer shifts (IS) ranging from 0.31 to 0.34 mm s^{-1}. These values are consistent with those obtained by Castelein et al. (2002) at RT for kaolinite (EQ = 0.58 mm s^{-1} and IS = 0.35 mm s^{-1}). Analyses of the quadrupole doublet line width (Γ) show values varying from 0.45 to 0.58 mm s^{-1}.

To analyze the spectra recorded at 20 K, it was necessary to add a sextet to the adjustment model proposed for the SSA and SPF samples and two sextets for the SV and SBJ samples (Fig. 4). Table 3 summarizes the hyperfine parameters obtained by the fitting procedure of these spectra. The EQ values for the paramagnetic doublet at 20 K have values

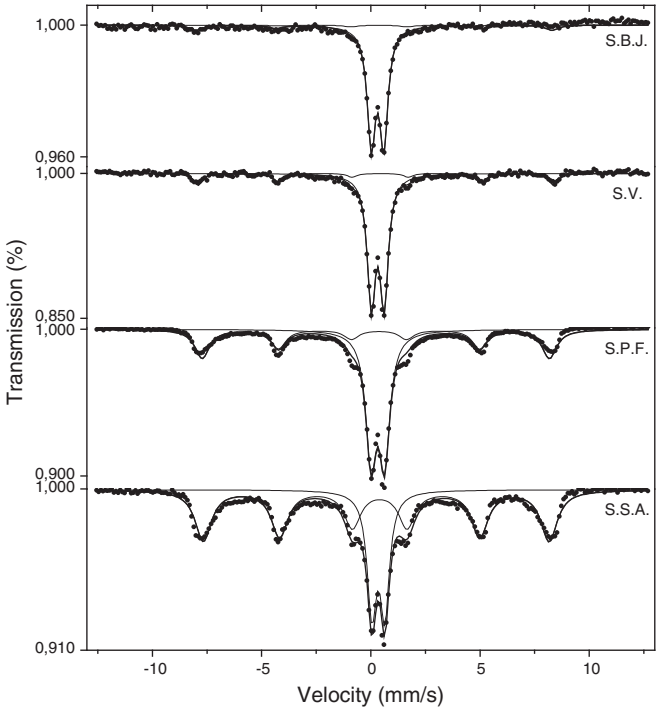

Fig. 3. Mössbauer spectroscopy spectra at room temperature (RT) conditions across an environmental gradient in southern Brazil. SBJ is the Bom Jesus site, SV is the Vacaria site, SPF is the Passo Fundo site, and SSA is the Santo Ângelo site.

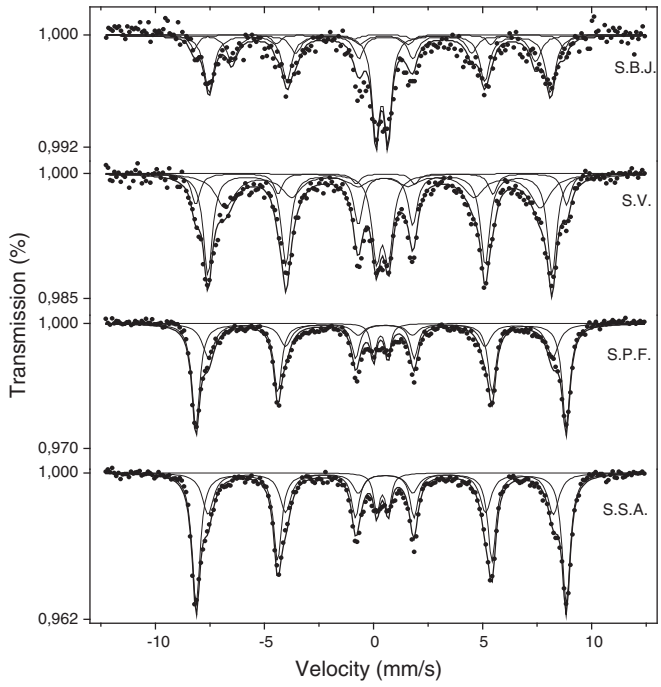

Fig. 4. Mössbauer spectroscopy spectra at 20 K temperature (20 K) conditions in the environmental gradient in southern Brazil. SBJ is the Bom Jesus site, SV is the Vacaria site, SPF is the Passo Fundo site, and SSA is the Santo Ângelo site.

similar to those obtained at RT for each sample. This outcome supports the interpretation that kaolinite is present in all soil samples, according to the XRD patterns (Fig. 2). The magnetic component of the spectra at RT can be well-fitted using a single sextet, and it provides values for the hyperfine parameters (Table 3) that are very close to those obtained for the hematite found in the sand and silt fractions of Brazilian Ferralsols (α-Fe_2O_3: $B_{hf} \approx 49$ T, EQ $= -0.18$ mm s^{-1}, IS $= 0.38$ mm s^{-1}), according to Ferreira et al. (2003). The large width line of the sextets indicates low crystallinity concomitant with high Al substitution in hematite. The hyperfine parameter values B_{hf} and EQ (Table 3) are associated with two sextets, and they are in agreement with those obtained by Wagner and Wagner (2004) for hematite ($B_{hf} = 53.5$ T, EQ $= -0.20$ mm s^{-1}) and goethite ($B_{hf} = 50.6$ T, EQ $= -0.25$ mm s^{-1}). This finding also confirms the presence of a wide particle size distribution.

The third sextet used to fit the Mössbauer spectra for the SV and SBJ samples show hyperfine magnetic field values of 43 and 49 T, and EQ $=$ 0 mm s^{-1}. This outcome could indicate the presence of ferrihydrite because of the poorly crystallized nanoparticles, according to Murad (2013). The soil samples contain nanostructured iron sesquioxide forms at 53.3% for the SPF site (doublet RT *minus* doublet 20 K), 61.1% for the SV site, and 67.8% for the SBJ of the total iron, and the SSA sample contains only 26.4%. The subspectral areas of the sextet corresponding to hematite was 61.1%, 62.4%, 11.1%, and 8.1% for the SSA, SPF, SV, and SBJ samples, respectively. The subspectral areas corresponding to the sextet for goethite was 32.3%, 30.3%, 46.5%, and 45.0% for the SSA, SPF, SV, and SBJ samples, respectively. However, the third sextet, corresponding to ferrihydrite, exhibited subspectral areas of 27.3% and 20.9% in the SV and SBJ samples, respectively. These outcomes demonstrate that the hematite is dominating the SSA and SPF samples, and goethite dominates the SV and SBJ samples. It is also important to note that in the SV and SBJ samples, the ferrihydrite was found in concentrations larger than that of hematite. The hematite content tends to increase with the decreasing of altitude ($r = -0.97$; $P < 0.05$) and OC content ($r = -0.96$; $P < 0.05$). Furthermore, ferrihydrite tends to increase with the increasing of OC ($r = 0.94$; $P = 0.06$) however they tend to decrease with the increasing of maximum air temperature across the environmental gradient ($r = -0.94$; $P = 0.06$). The goethite and ferrihydrite oxide content are related to the Fe_o content ($r = 0.91$; $P = 0.09$ and $r = 0.95$; $P < 0.05$).

Table 3
Mössbauer parameters at room temperature and at 20 K of the soil types across an environmental gradient in southern Brazil.

Sites	IS[a] mm s^{-1}	EQ[b] mm s^{-1}	B_{hf} T	Γ mm s^{-1}	Subspectral area %	Composition
Mössbauer parameters at room temperature						
SBJ: Bom Jesus	0.31	0.57		0.45	87.5	Doublet
	0.30	−0.22	50.6	0.73	12.5	Sextet
SV: Vacaria	0.32	0.59		0.45	82.9	Doublet
	0.33	−0.20	50.6	0.50	17.1	Sextet
SPF: Passo	0.32	0.61		0.58	60.6	Doublet
Fundo	0.30	−0.15	49.4	0.81	39.4	Sextet
SSA: Santo	0.34	0.59		0.51	33.0	Doublet
Ângelo	0.33	−0.16	49.2	0.91	67.0	Sextet
Mössbauer parameters at 20 K						
SBJ: Bom Jesus	0.38	0.55		0.40	26.0	Doublet
	0.38	−0.20	52.7	0.44	8.1	Hematite
	0.42	−0.26	48.6	0.55	45.0	Goethite
	0.45	0.00	43.2	0.70	20.9	Ferrihydrite
SV: Vacaria	0.41	0.55		0.45	15.1	Doublet
	0.45	−0.20	52.8	0.46	11.1	Hematite
	0.42	−0.26	49.0	0.50	46.5	Goethite
	0.42	0.00	44.9	1.09	27.3	Ferrihydrite
SPF: Passo	0.43	0.63		0.31	7.3	Doublet
Fundo	0.43	−0.18	52.7	0.43	62.4	Hematite
	0.43	−0.24	49.1	0.66	30.3	Goethite
SSA: Santo	0.41	0.52		0.33	6.6	Doublet
Ângelo	0.43	−0.17	52.7	0.44	61.1	Hematite
	0.44	−0.22	49.2	0.66	32.3	Goethite

IS is the isomer shift; EQ is the quadrupole splitting. B_{hf} is the hyperfine magnetic field; Γ is the Lorentzian linewidth.

3.3. Soil phosphorus sorption–desorption capacity along the environmental gradient

The total *P* values, expressed in mg kg^{-1} of soil, were low (<1615 mg kg^{-1} — Table 4) and close to the values found in the literature for tropical soils that generally ranged from 40 mg kg^{-1} (Kuczak et al., 2006) to 1426 mg kg^{-1} (Solomon et al., 2002). Moreover, available P was very low, representing only 0.3–2.4% of the total P

Table 4
Sesquioxide contents in soils samples collected across an environmental gradient in southern Brazil.

Soil attributes	Sites			
	Bom Jesus SBJ	Vacaria SV	Passo Fundo SPF	Santo Ângelo SSA
Sesquioxide contents[a]				
Hematite, g kg^{-1}	49	62	176	384
Goethite, g kg^{-1}	273	262	85	203
Ferrihydrite, g kg^{-1}	127	154	0	0
Gibbsite	Present	Present	–	–
P forms				
P (Mehlich-1), mg kg^{-1}[b]	12.3	12.0	10.7	4.8
P (AER), mg kg^{-1}[c]	14.0	17.0	18.7	5.2
P (AER), % of the total P	2.3	1.8	2.4	0.3
Total P, mg kg^{-1} soil[d]	611	961	786	1615
Recovered P, %[e]	142	162	345	153

[a] Values for soil iron oxides were calculated based on the results of the Mössbauer analysis and the clay content of each soil.
[b] Available P extracted by acid Mehlich-1 solution (0.05 mol L^{-1} HCl + 0.0125 mol L^{-1} H_2SO_4).
[c] Available P extracted in water by anion exchange resin membrane saturated with NaHCO3 0.5 mol L^{-1} at pH 8.5.
[d] Total P estimated by X-ray fluorescence method.
[e] Amount of P adsorbed recovered by successive resin extractions.

(Table 4). This finding is in agreement with the parent material composition and weathering status of the soils.

After contact the soil with 600 mg kg^{-1} of P during three days, it was performed the successive extractions with anion exchange resin. After five P extractions the P desorption curves reached a plateau and afterwards, very little additional P was extracted from the soil (Fig. 5). The SPF site showed the lowest content of readily and potentially available P. The amount of adsorbed P recovered by successive resin extractions was approximately two times higher in the SPF site (345%) than in the other soils (152% on average) (Table 4). Recovering capacity was higher than the amount of P fixed indicating desorption of native P with the successive resin extractions. The amount of native P desorbed by successive resin extractions was 39, 29, 38, and 14% of the total P for SBJ, SV, SPF, and SA, respectively. This amount of native P desorbed tends to increase with the increasing of the percentage of total P available P by AER ($r = 0.99$; $P = 0.008$). Through the adjustment to the clay content, the SPF site also showed the lowest level of adsorbed P, but it had the highest values of readily and potentially available P (Figs. 5 and 6). Despite the highest total P content in the SSA site (Table 4), this soil adsorbed the highest quantities of P and had the lowest values of desorbed P in the first (α) and potentially available P (Fig. 6).

The remaining (Prem) values ranged from 4 to 47.8 mg L^{-1} (Fig. 6). The SPF site had a higher Prem value (47.8 mg L^{-1}) and a lower fixed P (122.5 mg kg^{-1}), and the SBJ sample had the lowest Prem (4.0 mg L^{-1}) and the highest P-fixed value (559.9 mg kg^{-1}) (Fig. 6).

The total P content tends to increase with the increasing of Fe_d levels ($r = 0.91$; $P = 0.08$). The soil clay content attribute alone tends to explain a negative relationship with Prem and recovered P ($r = -0.94$; $P = 0.06$ and $r = -0.99$; $P < 0.01$). In addition, this attribute tends to have a positive relationship with the fixed P and α parameter ($r = 0.90$; $P = 0.09$ and $r = 0.96$; $P < 0.05$). Goethite seemed to have the greatest influence on P sorption ($r = -0.97$; $P < 0.05$). Similar to the clay content, the goethite content explains the relation between Prem and recovered P, with coefficients of $r = -0.97$ ($P < 0.05$) and $r = -0.94$ ($P = 0.06$), respectively. Goethite positively explains the results of the α and β parameters, with coefficients of $r = 0.97$ ($P < 0.05$) and $r = 0.99$ ($P < 0.01$), respectively. The contents of Fe_o and Fe_d showed no relationship with any P adsorption and desorption parameters, but the Fe_o/Fe_d ratio showed high negative correlation with the easily desorbable P ratio ($r = -1.00$; $P < 0.01$).

4. Discussion

Across the environmental gradient, the elevation, temperature, and rainfall regime were the primary sensitive topo-climatic factors (Table 1). As the altitude increases from west to east, a slight increase was observed in the rainfall regime, and the air temperature decreased slightly. This set of conditions primarily resulted in an increase in the soil OC content as well as the Fe_o/Fe_d ratios and decreased Fe_d–Fe_o values (Table 2). Crystallized Fe oxide (Fe_d) was predominant in all soils along the environmental gradient; however, the occurrence of hematite, goethite, and ferrihydrite varied as indicated by the Fe_o/Fe_d ratios. The hematite content decreased along the environmental gradient from west to east, and the ferrihydrite (estimated by Mössbauer spectroscopy) and gibbsite (estimated by XRD) only appear in the sites at the highest elevation > 900 m asl (SV and SBJ) (Tables 1 and 2). The occurrence of ferrihydrite was observed when the Fe_o/Fe_d ratios were higher than 0.13. Gibbsite occurred together with ferrihydrite, as also reported by Wada and Aomine (1966) in volcanic-ash soils.

$R^{3+}/R^{3+}+R^{2+}+M^{+}$ values higher than 0.9 and with low base content (Table 2) confirm that soils located at low altitudes (<590 m a.s.l.) are highly weathered. Despite the fact that all of the soils were highly weathered, as demonstrated by the weathering indices in Table 2, the OC content, qualitative and quantitative distribution of iron and aluminum sesquioxides varied markedly across the environmental gradient. For instance, the hematite content decreased with the altitude at higher rainfall and OC content, and it increased with higher temperatures at low elevations (Tables 1, 3, and 4). Conversely, goethite and ferrihydrite showed inverse relations because the factors that promote hematite formation are the same as those that inhibited ferrihydrite and goethite formation (Schwertmann and Kämpf, 1983). In addition, high OC content may induce occasional reducing conditions that favor the formation of goethite and inhibit hematite formation (Orrutea et al., 2012) or promote its preferential dissolution (Jeanroy et al., 1991). Thus, the SBJ and SV sites located at the highest elevations preferentially contained goethite and ferrihydrite compared with hematite. The SSA and SPF sites located at the lower elevation contained higher hematite content, and no ferrihydrite and gibbsite were found (Tables 3 and 4).

All soils exhibited a high potential to adsorb P (Fig. 6), which was favored by the low soil pH, high clay and sesquioxide contents. The P adsorption is primarily explained by the soil clay fraction contents, and goethite content when it was adjusted to amounts of clay fraction (Tables 1 to 3, and Fig. 6). Nevertheless, soils containing similar clay content, i.e., SBJ and SSA, but located in the opposite sites along the environmental gradient, adsorbed different amounts of P (Table 1, and Fig. 6). This behavior can be associated with the OC content and/or iron–aluminum oxide content. It is well known that soils with high total concentrations of organic carbon may decrease the P adsorption sites through competition exerted by organic acids of low molecular weights (Redel et al., 2007). However, even with an OC content that was 1.8 times higher than that of the SSA soil, the SBJ soil showed a phosphorus adsorption capacity that was 1.3 times higher. This finding indicates that the iron–aluminum sesquioxide species play, here, a major role in soil adsorption–desorption phenomena, and OC acts indirectly on these species, determining the proportion of iron forms (Fe_o/Fe_d and sesquioxide species soil composition). In addition, the SBJ and SV soils located at high altitudes and containing a similar iron–aluminum sesquioxide assemblage (Tables 3 and 4) showed a high ability to adsorb P (P-fixed) followed by the SSA and SPF sites (Fig. 6). Regarding the P adsorption and desorption adjusted to the clay fraction content, the highest P fixation was also found in the SBJ soil, following the SV and SSA soils. The SPF soil had the lowest P adsorption, but it contained the highest amount of desorbed P as adjusted to the clay content (Fig. 6). Thus, the P behavior (regardless of the organic matter content) indicates that iron-Al sesquioxide species adsorbed and desorbed P differently. The soil's ability to desorb P was accurately predicted by both clay and goethite content because their high positive correlation coefficient.

In general, the soils exhibited high amounts of labile and potentially labile P (α and β; Fig. 6). The SSA, SV, and SBJ soils desorbed an average of 152% of the previously adsorbed P (Table 4), indicating total

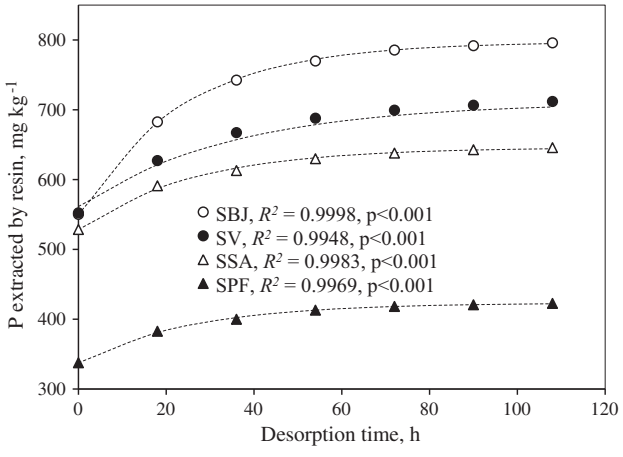

Fig. 5. Cumulative phosphorus (P) desorbed by successive anion exchange resin extractions. These samples were taken from P-saturated soils across an environmental gradient in southern Brazil. SBJ is the Bom Jesus site, SV is the Vacaria site, SPF is the Passo Fundo site, and SSA is the Santo Ângelo site.

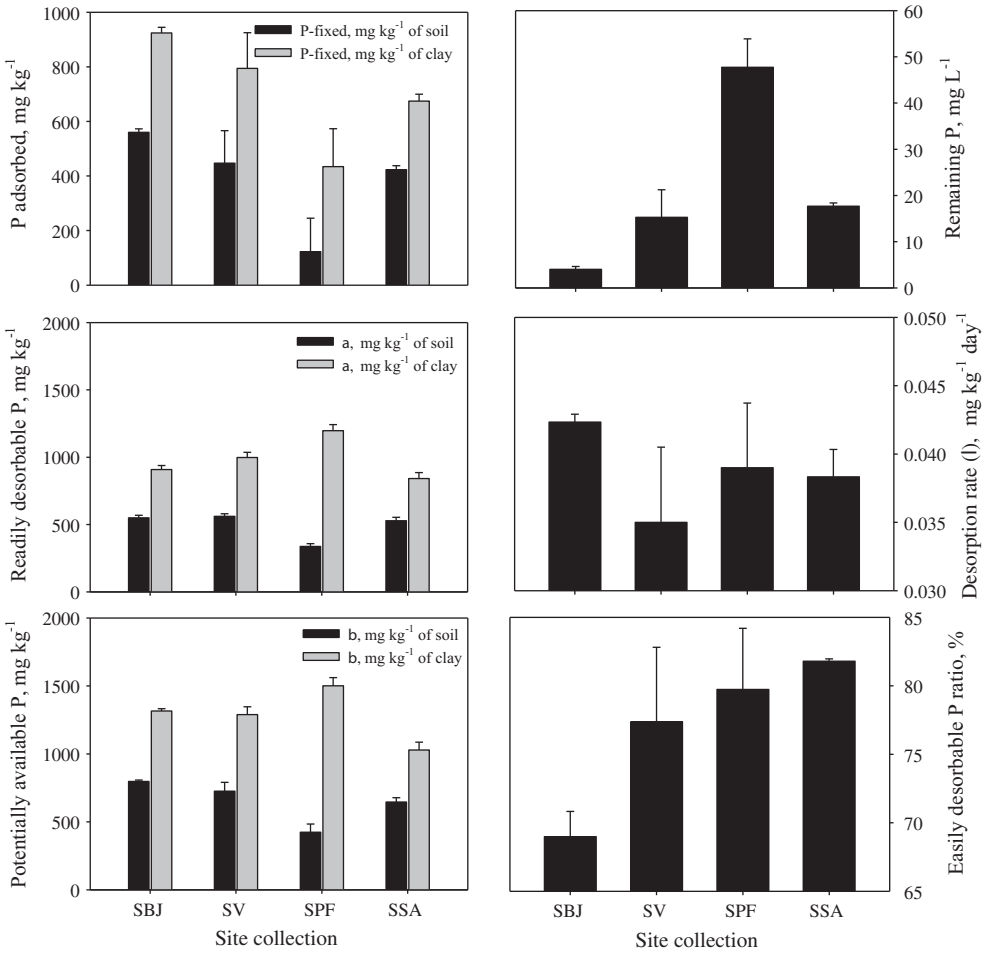

Fig. 6. Soil P sorption desorption parameters. SBJ is the Bom Jesus site, SV is the Vacaria site, SPF is the Passo Fundo site, and SSA is Santo Ângelo. Remaining P (Prem) according to Alvarez et al. (2000); α, is the readily desorbable P (labile P); β is the potentially available P (potentially available P); λ is the constant desorption rate of the first-order desorption reaction.

desorption of the P added plus part of the native P of the soils. However, the SPF desorbed 3.45 times the amount of adsorbed P, meaning that this soil desorbed much more native P than the others soils. This finding was primarily attributed to the low level of goethite soil content. These results corroborated with the findings of Guzman et al. (1994), who found that the P bioavailability is dependent on the nature of the iron (hydr)oxides, and the P adsorbed by ferrihydrite and hematite is more bioavailable than that adsorbed by goethite. Because ferrihydrite exhibits poor crystallinity and high micropore volume (Wang et al., 2013), it is expected to have a high phosphate adsorption and low phosphate desorption. The SBJ and SV soils presented a similar sesquioxide species assemblage, and they were the only ones that presented ferrihydrite content. However, there was no correlation between ferrihydrite and the amounts of P adsorbed and desorbed. It can be explained because under natural conditions, part of the ferrihydrite may be already interacting with the soil organic matter, blocking the P adsorption sites. If these soils are included in cropping systems with a decline of soil organic matter content, the P adsorption sites of ferrihydrite will become available, and then they will adsorb larger amount of P, which in turns will affect directly the amount of P fertilizer required to cultivate theses soils.

5. Conclusions

This study showed that the environmental gradient conditions in a Brazilian subtropical climate determine the qualitative and quantitative occurrence of iron and aluminum oxy-hydroxides, even in soils with pedogenic processes of intense weathering. These substantial differences in turn have a significant influence on the soil P adsorption and desorption capacities.

The variation in altitude along the environmental gradient promotes decreases in hematite, which were associated with the occurrence of goethite and ferrihydrite because of the Fe_o/Fe_d and total organic carbon content increases. In addition, soils from high altitudes (>900 m asl) preferentially contain goethite, ferrihydrite, and gibbsite, and the hematite species is preferentially found at low altitudes. The clay content allows a good prediction of the soil P adsorption and desorption capacities. Furthermore, the soil's ability to desorb P is also predicted by goethite content.

Finally, even across an apparently smooth environmental gradient, the variations in soil sesquioxide minerals as well as the dynamic of theses after changes in soil organic matter contents due to soil crops should be taken into account for adequate P fertilization and the potential P transfer from soils to aquatic systems.

Acknowledgments

The authors thank the CAPES (CAPES-COFECUB program, 009/2011, process number 3504-11-5) for financial support, as well as M. A. Santanna for her support in the soil P analysis. E. C. Bortoluzzi, CNPq researcher (Brasilia/Brazil), thanks CAPES-Brazil for the post-doctoral fellowship accorded by (8709-12-2) and UPF for the LPG program.

References

Alvarez, V.V.H., Novais, R.F., Dias, L.E., Oliveira, J.A., 2000. Determinação e uso do fósforo remanescente. Boletim Informativo da Sociedade Brasileira de Ciência do Solo. 25, 27–32.

Barrow, N.J., 1983. A discussion on the methods of measuring the rate of reaction between soil and phosphate. Fertil. Res. 4, 51–61.

Blakemore, L.C., Searle, P.L., Daly, B.K., 1987. Methods for Chemical Analysis of Soils, New Zealand, Soil Bureau, Scientific Report 80.

Bortoluzzi, E.C., Velde, B., Pernes, M., Dur, J.C., Tessier, D., 2008. Vermiculite, with hydroxy-aluminium interlayer, and kaolinite formation in a subtropical sandy soil from south Brazil. Clay Miner. 43, 185–193.

Bortoluzzi, E.C., Rheinheimer, D.S., Santanna, M.A., Caner, L., 2013. Mineralogy and nutrient desorption of suspended sediments during a storm event. J. Soils Sediment. 13, 1093–1105.

Caner, L., Radtke, L.M., Vignol-Lelarge, M.L., Inda, A.V., Bortoluzzi, E.C., Mexias, A.S., 2014. Basalt and rhyo-dacite weathering and soil clay formation under subtropical climate in southern Brazil. Geoderma 235–236, 100–112.

Carter, D.L., Heiman, R., Gonzales, C.L., 1965. Ethylene glycol monoethyl ether for determining surface area of silicate minerals. Soil Sci. 100, 356–360.

Castelein, O., Aldon, L., Olivier-Fourcade, J., Jumas, J.C., Bonnet, J.P., Blanchart, P., 2002. ^{57}Fe Mossbauer study of iron distribution in a kaolin raw material: influence of the temperature and the heating rate. J. Eur. Ceram. Soc. 22, 1767–1773.

Chintala, R., Schumacher, T.E., McDonald, L.M., Clay, D.E., Malo, D.D., Papiernik, S.K., Clay, S.A., Julson, J.L., 2014. Phosphorus sorption and availability from biochars and soil/biochar mixtures. Clean — soil, air. Water 42, 626–634.

Comissão de Química e Fertilidade do Solo — CQFS-RS/SC, 2004. Manual de adubação e de calagem para os Estados do Rio Grande do Sul e Santa Catarina. (Liming and Fertilizing Manual for Rio Grande do Sul and Santa Catarina States). SBCS/NRS, Porto Alegre, Rio Grande do Sul, Brazil.

De Mesquita Filho, M.V., Torrent, J., 1993. Phosphate sorption as related to mineralogy of a hydrosequence of soils from the Cerrado region (Brazil). Geoderma 58, 107–123.

Devau, N., Le Cadre, E., Hinsinger, P., Jaillard, B., Gérard, F., 2009. Soil pH controls the environmental availability of phosphorus: experimental and mechanistic modelling approaches. Appl. Geochem. 24, 2163–2174.

Dixon, J.E., Weed, S.B., 1989. Minerals in Soil Environments. Madison, Soil Science Society of America.

Ferreira, B.A., Fabris, J.D., Santana, D.P., Curi, N., 2003. Óxidos de ferro nas frações areia e silte de um Nitossolo desenvolvido de basalto. Rev. Bras. Ciênc. Solo 27, 405–413.

Guzman, G., Alcantara, E., Barron, V., Torrent, J., 1994. Phytoavailability of phosphate adsorbed on ferrihydrite, hematite and goethite. Plant Soil 159, 219–225.

Igwe, C.A., Zarei, M., Stahr, K., 2010. Fe and Al oxides distribution in some ultisols and inceptisols of southeastern Nigeria in relation to soil total phosphorus. Environ. Earth Sci. 60, 1103–1111.

IUSS Working Group, W.R.B., 2007. World reference base for soil resources 2006, first update 2007. World Soil Resources Reports No. 103. FAO, Rome.

Jeanroy, E., Rajot, J.L., Pillon, P., Herbillon, A.J., 1991. Differential dissolution of hematite and goethite in dithionite and its implication on soil yellowing. Geoderma 50, 79–94.

Kaminski, J., Rheinheimer, D.S., Bartz, H.R., 2001. Proposta de nova equação para determinação do valor de H + Al pelo uso do índice SMP em solos do RS e SC. (Proposal for a new equation for determining the value of H + Al by the use of SMP index in soil of Rio Grande do Sul and Santa Catarina States). Proceedings: Annual Meeting of Official Network of Laboratories in the States of Rio Grande do Sul and Santa Catarina States, Frederico Westphalen, Rio Grande do Sul State, Brazil.

Kämpf, N., Curi, N., Marques, J.J., 2009. Intemperismo e ocorrência de minerais no ambiente do solo. In: Melo, V.F., Alleoni, L.R.F. (Eds.), Química e mineralogia do solo — Parte I: Conceitos básicos. Sociedade Brasileira de Ciência do Solo, Viçosa, pp. 333–380.

Kim, J., Li, W., Philips, B.L., Grey, C.P., 2011. Phosphate adsorption on the iron oxyhydroxides goethite (α-FeOOH), akaganeite (β-FeOOH), and lepidocrocite (γ-FeOOH): a ^{31}P NMR study. Energy Environ. Sci. 4, 4298–4305.

Kuczak, C.N., Fernandes, E.C.M., Lehmann, J., Rondon, M.A., Luizão, F.J., 2006. Inorganic and organic phosphorus pools in earthworm casts (Glossoscolecidae) and a Brazilian rainforest Oxisol. Soil Biol. Biochem. 38, 553–560.

Lair, G.J., Zehetner, F., Khan, Z.H., Gerzabek, M.H., 2009. Phosphorus sorption–desorption in alluvial soils of a young weathering sequence at the Danube River. Geoderma 149, 39–44.

Li, W., Feng, X., Yan, Y., Sparks, D.L., Philips, B.L., 2013. Solid-state NMR spectroscopic study of phosphate sorption mechanisms on aluminum (hydr)oxides. Environ. Sci. Technol. 47, 8308–8315.

McKean, S.J., Warren, G.P., 1996. Determination of phosphate desorption characteristics in soils using successive resin extractions. Commun. Soil Sci. Plant Anal. 27, 2397–2417.

Mehra, J.P., Jackson, M.L., 1960. Iron oxides removal from soils and clays by a dithionite–citrate–bicarbonate system buffered with sodium bicarbonate. Clay Clay Miner. 7, 317–327.

Meunier, A., Caner, L., Hubert, F., Albani, A.E.L., Prêt, D., 2013. The weathering intensity scale (WIS): an alternative approach of the chemical index of alteration (CIA). Am. J. Sci. 313, 113–143.

Murad, E., 2013. Mössbauer spectroscopy. In: Bergaya, F., Lagaly, G. (Eds.), Handbook of Clay Science: Part B, Techniques and Applications, 2nd edition. 5B, pp. 11–24.

Murphy, J., Riley, J.P., 1962. A modified single solution method for the determination of phosphate in natural waters. Anal. Chim. Acta. 27, 3–36.

Orrutea, A.G., Melo, V.F., Motta, A.C.V., Lima, V.C., 2012. Mineralogia e reserva de K de Cambissolos submetidos a diferentes manejos após derrubada e queima da floresta na Amazônia Meridional. Acta Amazon. 42, 461–470.

Paduani, C., Pérez, C.A.S., Gobbi, D., Ardisson, J.D., 2009. Mineralogical characterization of iron-rich clayey soils from the middle plateau in the southern region of Brazil. Appl. Clay Sci. 42, 559–562.

Rasmussen, C., Dahlgren, R.A., Southard, R.J., 2010. Basalt weathering and pedogenesis across an environmental gradient in the southern Cascade Range California, USA. Geoderma 154, 473–485.

Redel, Y.D., Rubio, R., Rouanet, J.L., Borie, F., 2007. Phosphorus bioavailability affected by tillage and crop rotation on a Chilean volcanic derived Ultisol. Geoderma 139, 388–396.

Rheinheimer, D.S., Campos, B.H.C., Giacomini, S.J., Conceição, P.C., Bortoluzzi, E.C., 2008. Comparação de métodos de determinação de carbono orgânico total no solo. Rev. Bras. Ciênc. Solo 32, 435–440.

SAS, 1992. Statistical Analysis System: Release 6.08 (Software). Cary: SAS Institute.

Shoemaker, H.E., Maclean, E.O., Pratt, P.F., 1961. Buffer methods for determining lime requirement of soils with appreciable amounts of extractable aluminum. Soil Sci. Soc. Am. Proc. 25, 274–277.

Schwertmann, U., Kämpf, N., 1983. Óxidos de ferro em ambientes pedogenéticos brasileiros. Rev. Bras. Ciênc. Solo 7, 251–255.

Schwertmann, U., Schulze, D.G., Murad, E., 1982. Identification of ferrihydrite in soils by dissolution kinetics, differential x-ray diffraction, and Mössbauer spectroscopy. Soil Sci. Soc. Am. J. 46, 869–875.

Solomon, D., Lehmann, J., Mamo, T., Fritzsche, F., Zech, W., 2002. Phosphorus forms and dynamics as influenced by land use changes in the sub-humid Ethiopian highlands. Geoderma 105, 21–48.

Tedesco, M.J., Giancelo, C., Bissani, C.A., Bohnen, H., Volkweiss, S.J., 1995. Análise, de solo, plantas e outros materiais. (Analisys of soil, plant and other materials), 1995, Soil Department, UFRGS; Porto Alegre. Rio Grande do Sul, Brazil.

Wada, K., Aomine, S., 1966. Occurrence of gibbsite in weathering of volcanic materials at Kuroishibaru, Kumamoto. Soil Sci. Plant Nutr. 12, 25–31.

Wagner, F.E., Wagner, U., 2004. Mössbauer spectra of clays and ceramics. Hyperfine Interactions. 154, 35–82.

Wang, X., Liu, F., Tan, W., Li, W., Feng, X., Sparks, D.L., 2013. Characteristics of phosphate adsorption–desorption onto ferrihydrite: comparison with well-crystalline Fe (hydr)oxides. Soil Sci. 178, 1–11.

Walkley, A., Black, I.A., 1934. An examination of the Degtjareff method for determining soil organic matter and a proposed modification of the chromic acid titration method. Soil Sci. 37, 29–38.

Wei, S.Y., Tan, W.F., Liu, F., Zhao, W., Weng, L.P., 2014. Surface properties and phosphate adsorption of binary systems containing goethite and kaolinite. Geoderma 213, 478–484.